Physics Letters B 816 (2021) 136266

Contents lists available at ScienceDirect

Physics Letters B

www.elsevier.com/locate/physletb

β-delayed neutron emission of r-process nuclei at the $N = 82$ shell closure

O. Hall [a,*], T. Davinson [a], A. Estrade [b], J. Liu [c,d], G. Lorusso [c,e,f], F. Montes [g], S. Nishimura [c], V.H. Phong [c,h], P.J. Woods [a], J. Agramunt [i], D.S. Ahn [c,j], A. Algora [i], J.M. Allmond [k], H. Baba [c], S. Bae [m], N.T. Brewer [k,l], C.G. Bruno [a], R. Caballero-Folch [n], F. Calviño [o], P.J. Coleman-Smith [p], G. Cortes [o], I. Dillmann [n,q], C. Domingo-Pardo [i], A. Fijalkowska [r], N. Fukuda [c], S. Go [c], C.J. Griffin [a], R. Grzywacz [l], J. Ha [m,c], L.J. Harkness-Brennan [s], T. Isobe [c], D. Kahl [a], L.H. Khiem [t,u], G.G. Kiss [c,v], A. Korgul [r], S. Kubono [c], M. Labiche [p], I. Lazarus [p], J. Liang [w], Z. Liu [x,y], K. Matsui [c,z], K. Miernik [r], B. Moon [aa], A.I. Morales [i], P. Morrall [p], M.R. Mumpower [ab], N. Nepal [b], R.D. Page [s], M. Piersa [r], V.F.E. Pucknell [p], B.C. Rasco [k], B. Rubio [i], K.P. Rykaczewski [k], H. Sakurai [c,z], Y. Shimizu [c], D.W. Stracener [k], T. Sumikama [c], H. Suzuki [c], J.L. Tain [i], H. Takeda [c], A. Tarifeño-Saldivia [o], A. Tolosa-Delgado [i], M. Wolińska-Cichocka [ac], R. Yokoyama [l]

[a] School of Physics and Astronomy, University of Edinburgh, Edinburgh, EH9 3FD, UK
[b] Department of Physics, Central Michigan University, Mount Pleasant, MI, 48859, USA
[c] RIKEN Nishina Center, Wako, Saitama, 351-0198, Japan
[d] Department of Physics, University of Hong Kong, Pokfulman Road, Hong Kong
[e] National Physical Laboratory, Teddington, TW11 0LW, UK
[f] Department of Physics, University of Surrey, Guildford, GU2 7XH, UK
[g] National Superconducting Cyclotron Laboratory, East Lansing, MI, 48824, USA
[h] Faculty of Physics, VNU University of Science, Thanh Xuan, 120062 Hanoi, Vietnam
[i] Instituto de Física Corpuscular, CSIC and Universitat de Valencia, E-46980 Paterna, Spain
[j] Korea Basic Science Institute, 169-148, Gwahak-ro, Yuseong-gu, Daejeon, 34133, Republic of Korea
[k] Oak Ridge National Laboratory, Physics Division, TN 37831-6371, USA
[l] University of Tennessee, Knoxville, TN, USA
[m] Seoul National University, Department of Physics and Astronomy, Seoul 08826, Republic of Korea
[n] TRIUMF, Vancouver BC, V6T 2A3, Canada
[o] Universitat Politecnica de Catalunya, E-08028 Barcelona, Spain
[p] STFC Daresbury Laboratory, Daresbury, Warrington, WA4 4AD, UK
[q] Department of Physics and Astronomy, University of Victoria, Victoria BC, V8P 5C2, Canada
[r] Faculty of Physics, University of Warsaw, PL02-093 Warsaw, Poland
[s] Department of Physics, University of Liverpool, Liverpool, L69 7ZE, UK
[t] Institute of Physics, Vietnam Academy of Science and Technology, Ba Dinh, 118011 Hanoi, Vietnam
[u] Graduate University of Science and Technology, Vietnam Academy of Science and Technology, Cau Giay, 122102 Hanoi, Vietnam
[v] MTA Atomki, Debrecen, H4032, Hungary
[w] McMaster University, Department of Physics and Astronomy, Hamilton ON, L8S 4M1, Canada
[x] Institute of Modern Physics, Chinese Academy of Sciences, Lanzhou 730000, China
[y] School of Nuclear Science and Technology, University of Chinese Academy of Sciences, Beijing 100049, China
[z] University of Tokyo, Department of Physics, Tokyo 113-0033, Japan
[aa] Korea University, Department of Physics, Seoul 136-701, Republic of Korea
[ab] Theoretical Division, Los Alamos National Laboratory, Los Alamos, NM, 87544, USA
[ac] Heavy Ion Laboratory, University of Warsaw, Pasteura 5A, PL-02-093 Warsaw, Poland

ARTICLE INFO

Article history:
Received 10 December 2020
Received in revised form 29 March 2021

ABSTRACT

Theoretical models of β-delayed neutron emission are used as crucial inputs in r-process calculations. Benchmarking the predictions of these models is a challenge due to a lack of currently available experimental data. In this work the β-delayed neutron emission probabilities of 33 nuclides in the

* Corresponding author.
E-mail address: oscar.hall@ed.ac.uk (O. Hall).

https://doi.org/10.1016/j.physletb.2021.136266

Accepted 29 March 2021
Available online 1 April 2021
Editor: D.F. Geesaman

Keywords:
β-delayed neutron emission
r-process

important mass regions south and south-west of ^{132}Sn are presented, 16 for the first time. The measurements were performed at RIKEN using the Advanced Implantation Detector Array (AIDA) and the BRIKEN neutron detector array. The P_{1n} values presented constrain the predictions of theoretical models in the region, affecting the final abundance distribution of the second r-process peak at $A \approx 130$.

The astrophysical conditions for the r-process, i.e. the nucleosynthesis process responsible for the production of half the elements heavier than iron, are still a matter of debate [1–3]. Recent observations, such as the gravitational wave event GW170817 and its accompanying electromagnetic counterpart [4–8], point to binary neutron star mergers as a significant source of r-process material in the galaxy [8–10]. It is not yet determined whether these events are partially or entirely able to reproduce the r-process abundance pattern observed throughout the galaxy. Hydrodynamical models of these events [11] provide the astrophysical conditions present during these events, allowing reaction networks to simulate the nucleosynthesis taking place under explosive conditions [12]. Performing accurate reaction network calculations requires a precise knowledge of the nuclear properties of the nuclei involved. In particular, heavy element abundance predictions are sensitive to the values of nuclear masses, β-decay half-lives and β-delayed neutron emission probabilities P_n of very neutron-rich nuclei [13,14]. r-process calculations are not only sensitive to P_n values of nuclei along the r-process path but also of nuclei encountered as they β-decay back to stability, where neutron emission causes branching along the decay chains modifying the final abundance distributions and acts as a secondary source of neutrons during freeze-out.

Nuclear theory predictions of P_n values depend on the β-strength function S_β [15], and the masses of the nuclei used for the calculations. Theoretical models broadly fall into two categories: microscopic models and phenomenological models. Microscopic models aim to describe S_β based on microscopic theories, typically through some form of Quasiparticle Random Phase Approximation (QRPA) [16,17]. Phenomenological models aim to provide a description of S_β based on the systematic trends of existing experimental β-decay properties [18,19]. The benchmarking of these theoretical models against new experimental data, as they are extrapolated far from stability, is critical for reliable modelling of the astrophysical r-process [2,20]. When compared to the most recent evaluation of P_n values [21] microscopic models, such as the Finite Range Droplet Model with QRPA (FRDM+QRPA) [22], systematically underpredict the P_n values of nuclei in the mass region south-west of ^{132}Sn, just below the $N = 82$ shell closure. Sensitivity studies have shown r-process abundances to be particularly sensitive to changes in P_n values in this region that shapes the second r-process peak [14]. In this region the total P_n value for most nuclei is equal to its P_{1n} value, the probability of a single delayed-neutron being emitted.

In this paper the β-delayed neutron emission probabilities and β-decay half-lives of 33 neutron-rich nuclei with $N \leq 82$ are presented. In particular, we report the first experimental P_{1n} measurements of 16 nuclides: $^{115-116}$Tc, $^{116-121}$Ru, $^{119-124}$Rh, ^{128}Pd and $^{127-129}$Cd. Also included, and often with higher precision than previous data, are measurements of $^{121-128}$Pd, $^{124-129}$Ag and ^{130}Cd that encompass the nuclides for which the current discrepancy between experiment and theory is observed.

The experiment was performed at the Radioactive Isotope Beam Factory (RIBF) [23], located at the RIKEN Nishina Centre in Japan. Exotic neutron-rich nuclei were produced by in-flight fission of a 50 pnA primary beam of ^{238}U accelerated to an energy of 345 MeV/u impinging on a ^{9}Be target. The fission products of interest were analysed using the BigRIPS separator [24,25]. Particle identification (PID) was performed using the $\Delta E - B\rho -$ TOF method [26] in the second stage of BigRIPS. The resulting PID plot is shown in Fig. 1. Contaminant events such as hydrogen-like ions are clearly separated from the fully stripped ions of interest even for the most neutron-rich nuclei. The identified ions of interest were delivered to the F11 experimental area at a rate of around 100 ions per second via the ZeroDegree spectrometer [25].

The Advanced Implantation Detector Array (AIDA) [27] was installed in the F11 experimental area and used for the measurements of implanted ions and their subsequent decays. AIDA comprised six 128×128 strip, 1 mm thick Double-sided Silicon Strip Detectors (DSSDs). High resolution positional information was obtained for implanted ions via energy signal matching from the strips of the front and rear sides of the detector. When the energy was deposited across multiple adjacent strips, total deposited energy was calculated summing the individual strip contributions. The overlapping area between the front and rear strips in which energies were recorded form a cluster localising the event, typically to a region of ~ 1 mm^2 in the x and y planes of the detector. Decay events in the detector were localised using the same methodology although clusters were observed to vary in size due to the higher penetrability of β particles. Correlations between implantation and decay events were performed by identifying events in which the area of the β-decay event cluster was overlapping with or adjacent to the area of an implantation event cluster. This definition of a correlation was found to maximise the β-detection efficiency while minimising random correlations [28,29].

β-delayed neutrons were detected using the BRIKEN neutron counter array [30,31], which consisted of 140 ^{3}He proportional counters embedded in a High-Density Polyethylene (HDPE) matrix. A nominal neutron detection efficiency of 66.8(20)% was used for β-delayed neutrons in this region of interest. The efficiency was determined via the use of Monte Carlo simulations [30], and verified through measurements of the well-known neutron energy spectrum of ^{252}Cf [32]. Theoretical predictions of the neutron-energy spectra expected were obtained for two of the most neutron-rich nuclides studied, ^{124}Rh and ^{129}Ag. The spectra were generated utilising the model detailed in Ref. [33] and took S_β from Ref. [17]. These spectra showed that the majority of neutrons are predicted to be emitted in the energy range of $0-2$ MeV with average neutron energies of less than 1 MeV. Across this energy range the neutron-detection efficiency of BRIKEN is "flat", down to neutron energies of 0.1 keV [30,32], allowing the same nominal neutron-detection efficiency to be used for all nuclides.

Half-lives and P_{1n} values were obtained through simultaneous Bateman equation fits [34] of the β-decay and neutron-gated β-decay activities, which included the contributions of all decay products along the path to stability. The fits accounted for the contributions of random neutrons and random β-decay correlations. Fig. 2 shows an example fit of the neutron-gated activity of ^{121}Rh. A detailed description of the full analysis methodology used can be found in Ref. [32]. All values that were not measured in this experiment were taken from the Evaluated Nuclear Structure Data File (ENSDF) database [35].

The P_{1n} values and half-lives for nuclides measured in this work are presented in Table 1. Where upper limits have been assigned to a P_{1n} value, it is calculated with a 95% confidence

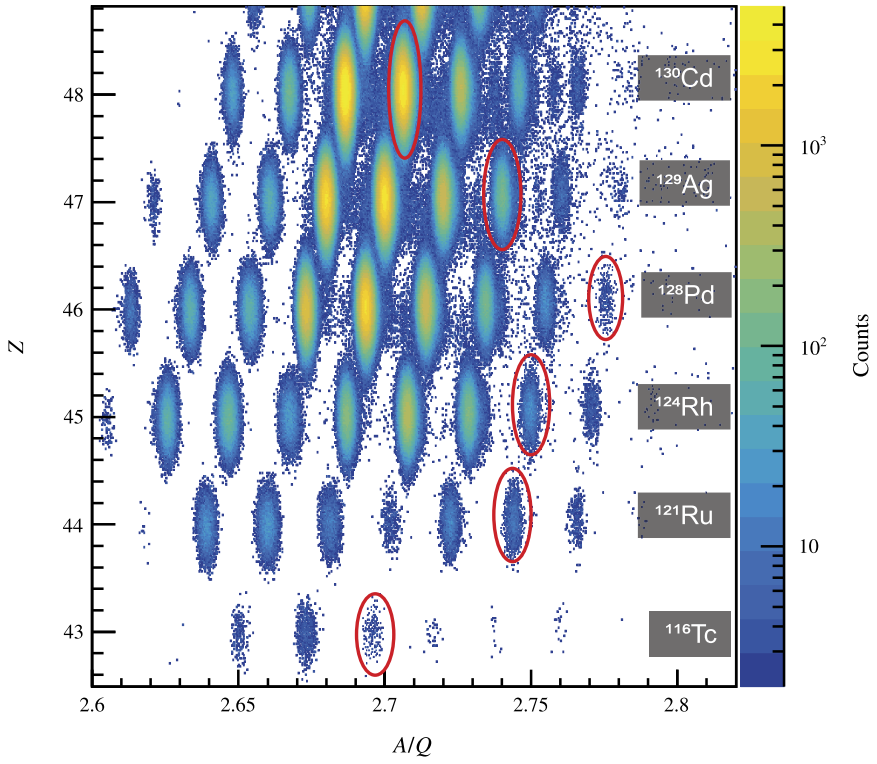

Fig. 1. Particle identification plot obtained by BigRIPS showing the atomic number Z against A/Q ratio of ions implanted in the AIDA detector stack. Nuclide labels relate to the adjacent groups highlighted by red ellipses.

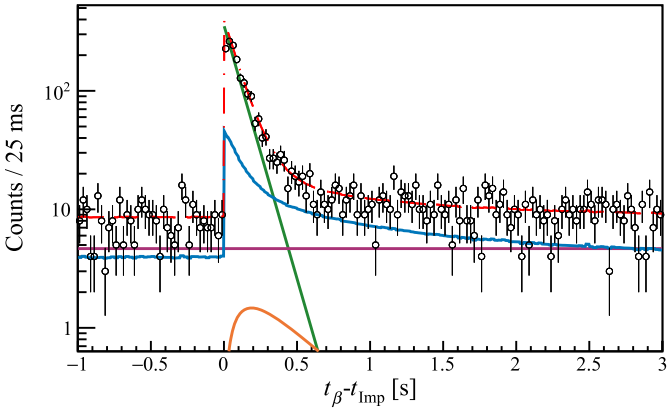

Fig. 2. Time distribution of neutron-gated ^{121}Rh β-decay events fitted as part of the analysis. The fitted function (red dashed line) includes contributions of the parent decay (green line), β-delayed neutron emitting daughters and granddaughters (orange line), randomly correlated neutrons (blue line) and a linear random background (purple line).

limit assuming a Gaussian estimator. Estimated masses extrapolated from the mass surface [36] indicate β-delayed two neutron emission may be energetically possible for several of the nuclei studied in the present work (indicated in Table 1). However, no evidence of two neutron emission was observed in this work. It should be noted that isomers are expected to be present in this region and that β-decaying isomers have previously been observed for some of the nuclei studied here, see for example, refs. [37,38]. A signature of the contribution of isomers in the present data would be the observation of more than one component in the decay curves, however, it was found that a single component for the parent decay gave the best fit result in all cases. As such only a single half-life and P_{1n} value is given for each nuclide.

Fig. 3 shows our measured P_{1n} values grouped by element as a function of neutron number. Recommended P_{1n} values from the recent evaluation [21] are also shown in Fig. 3. Predictions of four theoretical model calculations are included. These include the Finite Range Droplet Model [39] with the Quasiparticle Random Phase Approximation (FRDM+QRPA) [22], the FRDM+QRPA with the inclusion of a Hauser-Feshbach framework (FRDM+QRPA+HF) [17], the Relativistic Hartree-Bogoliubov mass model with the proton-neutron Relativistic QRPA [40] (RHB+*pn*-RQRPA) and the semi-empirical Effective Density Model [41,42].

When comparing the P_{1n} values from the most recent evaluation [21] to both the P_{1n} values presented here and those predicted by theory, significant discrepancies can be seen in Fig. 3. The evaluation values which show the largest systematic differences, $^{123-127}$Pd and $^{125-128}$Ag, are all taken from a single source, corresponding to a PhD thesis [43] representing the only available source of measurements for these nuclides and labelled as "preliminary" in [21]. The two other sources that make up the evaluation in the region — providing P_{1n} values for $^{118-121}$Rh, $^{121-122}$Pd and ^{124}Ag [44]; and ^{130}Cd [45] — are from peer reviewed sources and are consistent with the present, often more precise, values.

The P_{1n} values reported in this work show a regular trend for most elements, of increasing neutron emission probability as neutron number increases. Some odd-even staggering in the P_{1n} values is observed for the lighter elements, such as Tc, Ru and Rh, though this is seen to diminish for nuclei close to $Z = 50$ where a smoother increase is observed. The predictions of the FRDM+QRPA and FRDM+QRPA+HF calculations reproduce this trend well across all isotopic chains, matching much of the staggering that is observed in the experimental values. The P_{1n} values predicted by FRDM+QRPA (2003) are calculated using the "cutoff" method [22], making the assumption that if a state above the neutron-separation energy S_n of the β-decay daughter is populated a neutron will be emitted. With the inclusion of the HF framework, de-excitation of the daughter is handled statistically,

Table 1
β-delayed neutron emission probabilities P_{1n} and half-lives measured in the present work. The nuclides for which a $P1n$ value is reported for the first time are indicated by an asterisk (*). The nuclides for which β-delayed two neutron emission is predicted to be energetically possible [36] are indicated by a dagger (†).

Nuclide	P_{1n} [%]	Half-life [ms]	Nuclide	P_{1n} [%]	Half-life [ms]	Nuclide	P_{1n} [%]	Half-life [ms]
^{115}Tc*	19(5)	70(9)	^{121}Rh*	13.4(8)	73(2)	^{128}Pd*†	10(7)	52(10)
^{116}Tc*†	17(7)	64(16)	^{122}Rh*†	11.3(7)	52.4(15)	^{124}Ag	2.3(11)	205(17)
^{116}Ru*	<0.8	200(11)	^{123}Rh*†	24.2(14)	42.2(18)	^{125}Ag	2.2(11)	146(11)
^{117}Ru*	2.4(10)	162(9)	^{124}Rh*†	28(5)	35(3)	^{126}Ag	3.8(2)	103.2(14)
^{118}Ru*	<4.6	98(10)	^{121}Pd	<1.7	290(20)	^{127}Ag	5.5(2)	89.1(9)
^{119}Ru*†	6(5)	57(13)	^{122}Pd	<2.2	203(12)	^{128}Ag†	9.3(5)	67.4(16)
^{120}Ru*	6(3)	48(7)	^{123}Pd	1.4(3)	114(2)	^{129}Ag†	17.9(14)	55(3)
^{121}Ru*†	13(4)	37(5)	^{124}Pd	0.89(20)	94(3)	^{127}Cd*	<1.2	340(30)
^{118}Rh	2.1(9)	294(17)	^{125}Pd	3.7(4)	64.4(17)	^{128}Cd*	<1.9	243(11)
^{119}Rh	3.4(9)	192(12)	^{126}Pd	4.9(9)	51(3)	^{129}Cd*	1.84(15)	155.9(13)
^{120}Rh†	7.2(16)	150(15)	^{127}Pd†	9(3)	39(5)	^{130}Cd	3.0(2)	134(3)

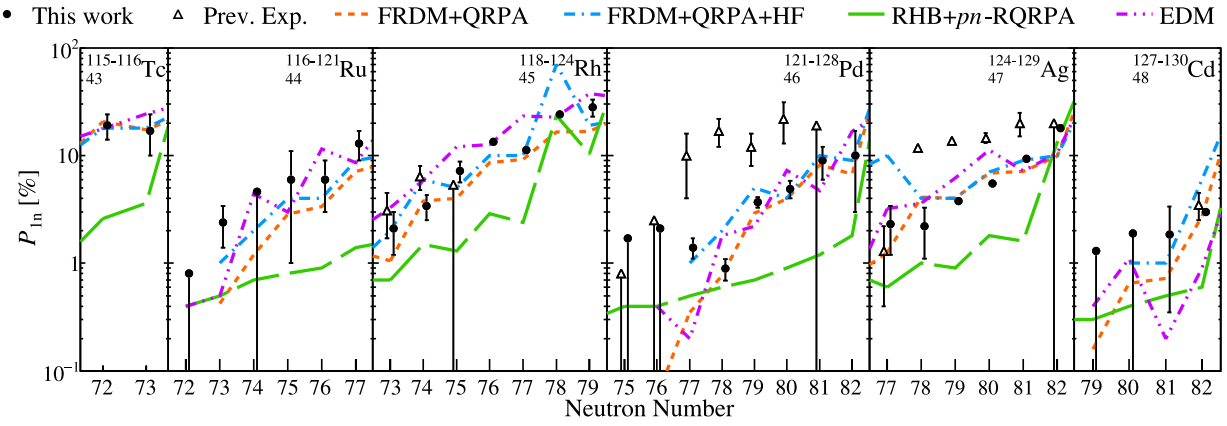

Fig. 3. Experimental P_{1n} values (symbols) from both this work (circles) and the current recommended values from the most recent evaluation [21] (triangles). Lines are used to show the published theoretical P_{1n}-values: FRDM+QRPA (orange line) [22], FRDM+QRPA+HF (blue line) [17], RHB+*pn*-RQRPA (green line) [40] and the EDM (purple line) [41,42].

including γ-ray emission explicitly at every stage [33,46]. The semi-empirical EDM calculations reproduce the general trend of the data well. Large odd-even staggering in the predicted P_{1n} values though result in the calculations fluctuating above and below the experimental values. The predictions of the RHB+*pn*-RQRPA are seen to be systematically smaller than both the predictions of the other models and the P_{1n} values measured here for almost all nuclides.

The impact of the newly measured P_{1n} values on *r*-process abundances was explored by estimating their effect during the decay to stability following the freeze-out of neutron-capture reactions. The calculation assumes that the *r*-process path passes through ^{128}Pd and ^{127}Rh, which act as classical waiting points with their abundances weighted by their respective half-lives, and that the decay to stability follows an instantaneous freeze-out. These isotones lying on the $N = 82$ shell closure are part of the *r*-process path in many calculations [47,48]. The resulting isobaric abundance distribution of the stable nuclei produced after the progenitor ^{128}Pd and ^{127}Rh abundances decay back to stability is shown in Fig. 4. The half-lives for ^{127}Rh and ^{128}Pd, used to calculate the seed abundances, were taken from Ref. [49]. Abundance uncertainties were calculated using a Monte Carlo approach where the experimental P_{1n} values from the present work were varied within their uncertainties. As it was not measured during the experiment, the P_{1n} value for ^{127}Rh was taken from the FRDM+QRPA+HF calculations [17], due to the model's good agreement with the measured values of other nuclei in the region (a factor of two uncertainty is assumed consistent with comparisons between experimental and predicted P_{1n} values in a recent evaluation [21]). The agreement observed between the theoretical P_{1n} values of FRDM+QRPA+HF and those presented in this work is reflected in the similar calculated abundances shown in Fig. 4. In contrast the large differences between the theoretical RHB+*pn*-RQRPA P_{1n} values and experiment are seen to have a significant impact on the abundance distribution, with large differences seen across all values of *A*.

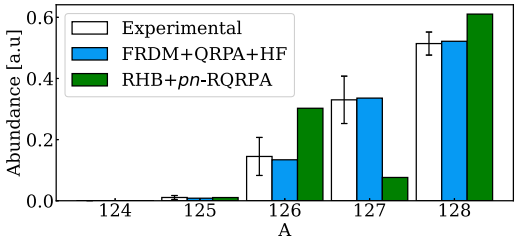

Fig. 4. Resulting *r*-process abundance following an instantaneous freeze out starting with an initial abundance distribution of ^{128}Pd and ^{127}Rh weighted by their literature half-lives.

Comparisons from our present calculations can be made with solar *r*-process abundances by taking the ratio of isobaric abundances *Y*. For example the $Y_{A=128}/Y_{A=127}$ ratio obtained with our experimental P_{1n} values, 1.56(38), compares with observations of the solar *r*-process abundance distribution which vary from $1.73 - 1.77$ [50–52]. The difference between the calculated and observed abundance ratios may be explained by the absence of $A = 129$ progenitor nuclei in the calculation. The $A = 129$ isobars ^{129}Ag and ^{129}Cd have P_{1n} values of 17.9(14)% and 1.84(15)%, respectively, resulting in around 18% of the final $A = 128$ abundance originating from the $A = 129$ decay chain. Accounting for this contribution in the abundances of $A = 128$ increases the ratio of $Y_{A=128}/Y_{A=127}$ to 1.9(5) in very good agreement with the observed solar ratio. In contrast, calculations using the predicted

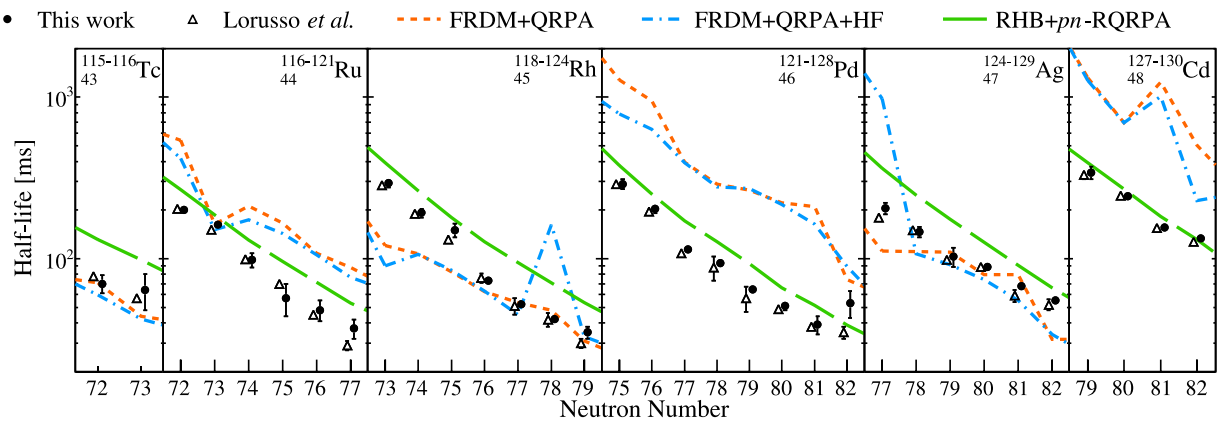

Fig. 5. Experimental half-lives (symbols) from both this work (circles) and Lorusso et al. [49] (triangles). Lines are used to show the published values of theoretical half-lives: FRDM+QRPA (orange line) [22], FRDM+QRPA+HF (blue line) [17] and RHB+*pn*-RQRPA (green line) [40].

P_{1n} values of RHB+*pn*-RQRPA result in a significantly larger ratio of 8.0, much larger than the observed solar ratio. These calculations show the importance of having precise P_{1n} values for use in *r*-process calculations, particularly in regions such as the $N = 82$ shell closure where large amounts of matter accumulate during the *r*-process allowing the P_{1n} values of relatively few nuclei to have a large impact on the final *r*-process abundance distribution. For example, the abundance of the long lived radioactive isotope of ^{129}I has been recently shown to be a key diagnostic tool in determining the site of origin for the *r*-process abundances in our solar system [53]. The P_{1n} values presented here, in particular those of ^{129}Ag and ^{129}Cd, will help to provide more reliable calculations of the amount of ^{129}I produced during *r*-process events. Reducing the uncertainties in these calculations will allow for tighter constraints to be placed on the conditions of the *r*-process event that most recently contributed to the *r*-process abundances observed.

Fig. 5 shows our measured β-decay half-lives grouped by element and plotted against neutron number. Recent literature half-lives from Lorusso et al. [49] are also shown for comparison. Excellent agreement is observed between the two data sets, with almost all values falling within uncertainties. When comparing these values with the predictions of theoretical models in Fig. 5, it is seen that the FRDM+QRPA calculations differ significantly from the measured half-lives, particularly for even-*Z* nuclides, in stark contrast to their good agreement with the measured P_{1n} values. The RHB+*pn*-RQRPA model best reproduces the nuclides presented here, despite systematically underpredicting the P_{1n} values of all nuclides. In particular, the RHB model calculations accurately reproduce the values for the Cd nuclides. The differences between the various models' abilities to predict P_n values and half-lives show the importance of having experimental measurements of both quantities to test the validity of these theoretical models as they are extrapolated far from stability.

In summary, we have presented β-delayed neutron emission probabilities and β-decay half-lives of 33 neutron-rich nuclei around the $N = 82$ shell closure of importance for the astrophysical *r*-process. Our new P_{1n} values are generally well reproduced by theoretical models. This agreement is in contrast with a significant discrepancy between the very recently published evaluation of P_n values [21] and the predictions of these theoretical models in the same region. Furthermore, we showed that while FRDM+QRPA calculations are able to reproduce the present P_{1n} values well, they are unable to reproduce the measured half-lives, in particular those of even-*Z* nuclides. In contrast RHB+*pn*-RQRPA calculations systematically under-predict P_{1n} values in this region, but are best able to reproduce the measured half-lives for the present nuclides. Calculations performed exploring the impact of P_{1n} values on the local astrophysical *r*-process abundance distribution show that the present P_{1n} values well explain the observed solar $A = 127$ and 128 abundances that form part of the second *r*-process peak.

Declaration of competing interest

The authors declare that they have no known competing financial interests or personal relationships that could have appeared to influence the work reported in this paper.

Acknowledgements

This experiment was performed at RI Beam Factory operated by RIKEN Nishina Center and CNS, University of Tokyo. O.H, T.D, P.J.W, C.G.B, C.J.G and D.K would like to thank STFC, UK for support. This research was sponsored in part by the Office of Nuclear Physics, U.S. Department of Energy under Award No. DE-FG02-96ER40983 (UTK) and DEAC05-00OR22725 (ORNL), and by the National Nuclear Security Administration under the Stewardship Science Academic Alliances program through DOE Award No. DENA0002132. This work was supported by National Science Foundation under Grants No. PHY-1430152 (JINA Center for the Evolution of the Elements), No. PHY-1565546 (NSCL), and No. PHY-1714153 (Central Michigan University). This work was supported by the Polish National Science Center under Contracts No. UMO-2015/18/E/ST2/00217, No. 2017/01/X/ST2/01144, No. 2019/33/N/ST2/03023 and No. 2020/36/T/ST2/00547. This work was also supported by JSPS KAKENHI (Grants No. 14F04808, No. 17H06090, No. 25247045, and No. 19340074). This work was also supported by Spanish Ministerio de Economía y Competitividad grants (FPA2011-06419, FPA2011-28770-C03-03, FPA2014-52823-C2-1-P, FPA2014-52823-C2-2-P, SEV-2014-0398, IJCI-2014-19172), by European Commission FP7/EURATOM Contract No. 605203, by the UK Science and Technology Facilities Council Grant No. ST/N00244X/1, by the National Research Foundation (NRF) in South Korea (No. 2016K1A3A7A09005575, No. 2015H1A2A1030275) and by the Natural Sciences and Engineering Research Council of Canada (NSERC) via the Discovery Grants SAPIN-2014-00028 and RGPAS 462257-2014. TRIUMF receives federal funding via a contribution agreement with the National Research Council Canada. This work was also supported by NKFIH (NN128072), and by the ÚNKP-20-5-DE-2 New National Excellence Program of the Ministry of Human Capacities of Hungary. G.G.K. acknowledges support from the Janos Bolyai research fellowship of the Hungarian Academy of Sciences. M.W.-C. acknowledges support from the Polish NCN project Miniatura No. 2017/01/X/ST2/01144. Z.L was supported by the National Key Research and Development Program of China (Contract

No. 2018YFA0404402), the National Natural Science Foundation of China (Grants No. 11961141004, No. 11735017, No. 11675225 and No. 11635003) and the Strategic Priority Research Program of Chinese Academy of Sciences (Grant No. XDB34000000). M.R.M. performed this work under the auspice of the U.S. Department of Energy at Los Alamos National Laboratory. Los Alamos National Laboratory is operated by Triad National Security, LLC, for the National Nuclear Security Administration of U.S. Department of Energy (Contract No. 89233218CNA000001).

References

[1] E.M. Burbidge, G.R. Burbidge, W.A. Fowler, F. Hoyle, Synthesis of the elements in stars, Rev. Mod. Phys. 29 (4) (1957) 547–650, https://doi.org/10.1103/RevModPhys.29.547.

[2] C.J. Horowitz, A. Arcones, B. Côté, I. Dillmann, W. Nazarewicz, I.U. Roederer, H. Schatz, A. Aprahamian, D. Atanasov, A. Bauswein, et al., *r*-process nucleosynthesis: connecting rare-isotope beam facilities with the cosmos, J. Phys. G, Nucl. Part. Phys. 46 (8) (2019) 083001, https://doi.org/10.1088/1361-6471/ab0849, arXiv:1805.04637.

[3] J.J. Cowan, C. Sneden, J.E. Lawler, A. Aprahamian, M. Wiescher, K. Langanke, G. Martínez-Pinedo, F.-K. Thielemann, Origin of the heaviest elements in the universe: The rapid neutron capture process, Rev. Mod. Phys. 93 (1) (2021) 015002, https://doi.org/10.1103/RevModPhys.93.015002, arXiv:1901.01410, http://arxiv.org/abs/1901.01410.

[4] B.P. Abbott, et al., LIGO Scientific Collaboration, V. Collaboration, GW170817: observation of gravitational waves from a binary neutron star inspiral, Phys. Rev. Lett. 119 (16) (2017) 161101, https://doi.org/10.1103/PhysRevLett.119.161101, arXiv:1710.05832.

[5] S.J. Smartt, T.-W. Chen, A. Jerkstrand, M. Coughlin, E. Kankare, S.A. Sim, M. Fraser, C. Inserra, K. Maguire, K.C. Chambers, et al., A kilonova as the electromagnetic counterpart to a gravitational-wave source, Nature (2017) 1–21, https://doi.org/10.1038/nature24303, arXiv:1710.05841.

[6] I. Arcavi, G. Hosseinzadeh, D.A. Howell, C. McCully, D. Poznanski, D. Kasen, J. Barnes, M. Zaltzman, S. Vasylyev, D. Maoz, S. Valenti, Optical emission from a kilonova following a gravitational-wave-detected neutron-star merger, Nature 551 (7678) (2017) 64–66, https://doi.org/10.1038/nature24291, arXiv:1710.05843.

[7] D.A. Coulter, R.J. Foley, C.D. Kilpatrick, M.R. Drout, A.L. Piro, B.J. Shappee, M.R. Siebert, J.D. Simon, N. Ulloa, D. Kasen, et al., Swope Supernova Survey 2017a (SSS17a), the optical counterpart to a gravitational wave source, Science 358 (6370) (2017) 1556–1558, https://doi.org/10.1126/science.aap9811, arXiv:1710.05452.

[8] D. Kasen, B. Metzger, J. Barnes, E. Quataert, E. Ramirez-Ruiz, Origin of the heavy elements in binary neutron-star mergers from a gravitational-wave event, Nature 551 (7678) (2017) 80–84, https://doi.org/10.1038/nature24453, arXiv:1710.05463.

[9] D. Watson, C.J. Hansen, J. Selsing, A. Koch, D.B. Malesani, A.C. Andersen, J.P.U. Fynbo, A. Arcones, A. Bauswein, S. Covino, et al., Identification of strontium in the merger of two neutron stars, Nature 574 (7779) (2019) 497–500, https://doi.org/10.1038/s41586-019-1676-3, arXiv:1910.10510, http://arxiv.org/abs/1910.10510%0A.

[10] R. Chornock, E. Berger, D. Kasen, P.S. Cowperthwaite, M. Nicholl, V.A. Villar, K.D. Alexander, P.K. Blanchard, T. Eftekhari, W. Fong, et al., The electromagnetic counterpart of the binary neutron star merger LIGO/Virgo GW170817. IV. Detection of near-infrared signatures of *r*-process nucleosynthesis with Gemini-South, Astrophys. J. 848 (2) (2017) L19, https://doi.org/10.3847/2041-8213/aa905c, arXiv:1710.05454.

[11] D.M. Siegel, B.D. Metzger, Three-dimensional general-relativistic magnetohydrodynamic simulations of remnant accretion disks from neutron star mergers: outflows and *r*-process nucleosynthesis, Phys. Rev. Lett. 119 (23) (2017) 1, https://doi.org/10.1103/PhysRevLett.119.231102.

[12] J. Lippuner, L.F. Roberts, SkyNet: a modular nuclear reaction network library, Astrophys. J. Suppl. Ser. 233 (2) (2017) 18, https://doi.org/10.3847/1538-4365/aa94cb, arXiv:1706.06198, http://arxiv.org/abs/1706.06198%0A.

[13] M.R. Mumpower, R. Surman, D.-L. Fang, M. Beard, P. Möller, T. Kawano, A. Aprahamian, Impact of individual nuclear masses on *r*-process abundances, Phys. Rev. C 92 (3) (2015) 035807, https://doi.org/10.1103/PhysRevC.92.035807, arXiv:1505.07789.

[14] M. Mumpower, R. Surman, G. McLaughlin, A. Aprahamian, The impact of individual nuclear properties on r-process nucleosynthesis, Prog. Part. Nucl. Phys. 86 (2016) 86–126, https://doi.org/10.1016/j.ppnp.2015.09.001, arXiv:1508.07352.

[15] H. Klapdor, The shape of the beta strength function and consequences for nuclear physics and astrophysics, Prog. Part. Nucl. Phys. 10 (C) (1983) 131–225, https://doi.org/10.1016/0146-6410(83)90004-2.

[16] P. Möller, J. Randrup, New developments in the calculation of β-strength functions, Nucl. Phys., Sect. A 514 (1) (1990) 1–48, https://doi.org/10.1016/0375-9474(90)90330-O.

[17] P. Möller, M. Mumpower, T. Kawano, W. Myers, Nuclear properties for astrophysical and radioactive-ion-beam applications (II), At. Data Nucl. Data Tables 125 (2019) 1–192, https://doi.org/10.1016/j.adt.2018.03.003.

[18] K. Takahashi, M. Yamada, Gross theory of nuclear β-decay, Prog. Theor. Phys. 41 (6) (1969) 1470–1503, https://doi.org/10.1143/PTP.41.1470.

[19] T. Tachibana, M. Yamada, Y. Yoshida, Improvement of the Gross theory of -decay. II: one-particle strength function, Prog. Theor. Phys. 84 (4) (1990) 641–657, https://doi.org/10.1143/ptp/84.4.641.

[20] J. Lippuner, L.F. Roberts, r-Process lanthanide production and heating rates in Kilonovae, Astrophys. J. 815 (2) (2015) 82, https://doi.org/10.1088/0004-637X/815/2/82, arXiv:1508.03133.

[21] J. Liang, B. Singh, E. McCutchan, I. Dillmann, M. Birch, A. Sonzogni, X. Huang, M. Kang, J. Wang, G. Mukherjee, et al., Compilation and evaluation of beta-delayed neutron emission probabilities and half-lives for $Z > 28$ precursors, Nucl. Data Sheets 168 (2020) 1–116, https://doi.org/10.1016/j.nds.2020.09.001.

[22] P. Möller, B. Pfeiffer, K.-L. Kratz, New calculations of Gross β -decay properties for astrophysical applications: speeding-up the classical r process, Phys. Rev. C 67 (5) (2003) 055802, https://doi.org/10.1103/PhysRevC.67.055802.

[23] Y. Yano, The RIKEN RI beam factory project: a status report, Nucl. Instrum. Methods Phys. Res., Sect. B, Beam Interact. Mater. Atoms 261 (1) (2007) 1009–1013, https://doi.org/10.1016/j.nimb.2007.04.174, the Application of Accelerators in Research and Industry.

[24] T. Kubo, K. Kusaka, K. Yoshida, A. Yoshida, T. Ohnishi, M. Ohtake, Y. Yanagisawa, N. Fukuda, T. Haseyama, Y. Yano, N. Kakutani, T. Tsuchihashi, K. Sato, Status and overview of superconducting radioactive isotope beam separator BigRIPS at RIKEN, IEEE Trans. Appl. Supercond. 17 (2) (2007) 1069–1077, https://doi.org/10.1109/TASC.2007.897203.

[25] T. Kubo, D. Kameda, H. Suzuki, N. Fukuda, H. Takeda, Y. Yanagisawa, M. Ohtake, K. Kusaka, K. Yoshida, N. Inabe, T. Ohnishi, A. Yoshida, K. Tanaka, Y. Mizoi, BigRIPS separator and ZeroDegree spectrometer at RIKEN RI beam factory, Prog. Theor. Exp. Phys. 2012 (1) (2012) 1–11, https://doi.org/10.1093/ptep/pts064.

[26] N. Fukuda, T. Kubo, T. Ohnishi, N. Inabe, H. Takeda, D. Kameda, H. Suzuki, Identification and separation of radioactive isotope beams by the BigRIPS separator at the RIKEN RI beam factory, Nucl. Instrum. Methods Phys. Res., Sect. B, Beam Interact. Mater. Atoms 317 (2013) 323–332, https://doi.org/10.1016/j.nimb.2013.08.048, arXiv:1310.8351.

[27] C. Griffin, T. Davinson, A. Estrade, D. Braga, I. Burrows, P. Coleman-Smith, T. Grahn, A. Grant, L.J. Harkness-Brennan, M. Kogimtzis, et al., β-decay studies of *r*-process nuclei using the advanced implantation detector array (AIDA), in: Proceedings of XIII Nuclei in the Cosmos — PoS(NIC XIII), 07-11-July, Sissa Medialab, Trieste, Italy, 2015, p. 097, https://pos.sissa.it/204/097.

[28] O. Hall, A. Estrade, J. Liu, G. Lorusso, K. Matsui, F. Montes, S. Nishimura, New implant-decay correlation method for β-delayed neutron emission measurements with the BRIKEN setup, RIKEN Accel. Prog. Rep. 52 (2019) 38.

[29] O. Hall, β-delayed neutron emission from *r*-process nuclei along the $N = 82$ shell closure, Ph.D. thesis, University of Edinburgh, 2020.

[30] A. Tarifeño-Saldivia, J. Tain, C. Domingo-Pardo, F. Calviño, G. Cortés, V. Phong, A. Riego, J. Agramunt, A. Algora, N. Brewer, et al., Conceptual design of a hybrid neutron-gamma detector for study of β-delayed neutrons at the RIB facility of RIKEN, J. Instrum. 12 (04) (Apr. 2017), https://doi.org/10.1088/1748-0221/12/04/P04006.

[31] J. Tain, J. Agramunt, D. Ahn, A. Algora, J. Allmond, H. Baba, S. Bae, N. Brewer, R. Caballero Folch, F. Calvino, et al., The BRIKEN project: extensive measurements of β-delayed neutron emitters for the astrophysical r process, Acta Phys. Pol. B 49 (3) (2018) 417, https://doi.org/10.5506/APhysPolB.49.417.

[32] A. Tolosa-Delgado, J. Agramunt, J. Tain, A. Algora, C. Domingo-Pardo, A. Morales, B. Rubio, A. Tarifeño-Saldivia, F. Calviño, G. Cortes, et al., Commissioning of the BRIKEN detector for the measurement of very exotic β-delayed neutron emitters, Nucl. Instrum. Methods Phys. Res., Sect. A, Accel. Spectrom. Detect. Assoc. Equip. 925 (2019) 133–147, https://doi.org/10.1016/j.nima.2019.02.004, arXiv:1808.00732.

[33] M.R. Mumpower, T. Kawano, P. Möller, Neutron-γ competition for β-delayed neutron emission, Phys. Rev. C 94 (6) (2016) 064317, https://doi.org/10.1103/PhysRevC.94.064317, arXiv:1608.01956v1.

[34] H. Bateman, The solution of a system of differential equations occurring in the theory of radioactive transformations, Proc. Camb. Philol. Soc. 15 (5) (1910) 423–427.

[35] National Nuclear Data Center, From ENSDF database as of 18th July 2019, Version available at http://www.nndc.bnl.gov/ensarchivals/. (Accessed December 2020).

[36] M. Wang, G. Audi, F.G. Kondev, W. Huang, S. Naimi, X. Xu, The AME2016 atomic mass evaluation (II). Tables, graphs and references, Chin. Phys. C 41 (3) (2017) 030003, https://doi.org/10.1088/1674-1137/41/3/030003.

[37] J.C. Batchelder, N.T. Brewer, C.J. Gross, R. Grzywacz, J.H. Hamilton, M. Karny, A. Fijalkowska, S.H. Liu, K. Miernik, S.W. Padgett, et al., Structure of low-lying states in ^{124,126}Cd populated by β decay of ^{124,126}Ag, Phys. Rev. C 89 (5) (2014) 054321, https://doi.org/10.1103/PhysRevC.89.054321.

[38] R. Dunlop, V. Bildstein, I. Dillmann, A. Jungclaus, C.E. Svensson, C. Andreoiu, G.C. Ball, N. Bernier, H. Bidaman, P. Boubel, et al., Half-lives of neutron-rich Cd128–130, Phys. Rev. C 93 (6) (2016), https://doi.org/10.1103/physrevc.93.062801.

[39] P. Möller, J.R. Nix, W.D. Myers, W.J. Swiatecki, Nuclear ground-state masses and deformations, At. Data Nucl. Data Tables 59 (2) (1995) 185–381, https://doi.org/10.1006/adnd.1995.1002, arXiv:nucl-th/9308022.

[40] T. Marketin, L. Huther, G. Martínez-Pinedo, Large-scale evaluation of β-decay rates of r-process nuclei with the inclusion of first-forbidden transitions, Phys. Rev. C 93 (2) (2016) 025805, https://doi.org/10.1103/PhysRevC.93.025805.

[41] K. Miernik, Phenomenological model of β-delayed neutron-emission probability, Phys. Rev. C 88 (4) (2013) 041301, https://doi.org/10.1103/PhysRevC.88.041301.

[42] K. Miernik, β-delayed multiple-neutron emission in the effective density model, Phys. Rev. C 90 (5) (2014) 054306, https://doi.org/10.1103/PhysRevC.90.054306.

[43] K.I. Smith, β Delayed Neutron Emission Studies of Neutron-Rich Palladium and Silver Isotopes, Ph.D. thesis, University of Notre Dame, 2014.

[44] F. Montes, A. Estrade, P.T. Hosmer, S.N. Liddick, P.F. Mantica, A.C. Morton, W.F. Mueller, M. Ouellette, E. Pellegrini, P. Santi, et al., β-decay half-lives and β-delayed neutron emission probabilities for neutron rich nuclei close to the $N = 82$ r-process path, Phys. Rev. C, Nucl. Phys. 73 (3) (2006), https://doi.org/10.1103/PhysRevC.73.035801.

[45] M. Hannawald, V. Fedoseyev, U. Köster, K.-L. Kratz, V. Mishin, W. Mueller, H. Ravn, J. Van Roosbroeck, H. Schatz, V. Sebastian, W. Walters, Decay properties of $n = 82$ to 84 cadmium r-process nuclides, Nucl. Phys. A 688 (1) (2001) 578–580, https://doi.org/10.1016/S0375-9474(01)00793-X, nuclei in the Cosmos.

[46] R. Yokoyama, R. Grzywacz, B.C. Rasco, N. Brewer, K.P. Rykaczewski, I. Dillmann, J.L. Tain, S. Nishimura, D.S. Ahn, A. Algora, et al., Strong one-neutron emission from two-neutron unbound states in β decays of the r-process nuclei Ga 86, 87, Phys. Rev. C 100 (3) (2019), https://doi.org/10.1103/PhysRevC.100.031302.

[47] J. Cowan, F. Thielemann, R-process nucleosynthesis in supernovae, Phys. Today 57 (10) (2004) 47–53, https://doi.org/10.1063/1.1825268.

[48] L.F. Roberts, J. Lippuner, M.D. Duez, J.A. Faber, F. Foucart, J.C. Lombardi, S. Ning, C.D. Ott, M. Ponce, The influence of neutrinos on r-process nucleosynthesis in the ejecta of black hole–neutron star mergers, Mon. Not. R. Astron. Soc. 464 (4) (2017) 3907–3919, https://doi.org/10.1093/mnras/stw2622.

[49] G. Lorusso, S. Nishimura, Z.Y. Xu, A. Jungclaus, Y. Shimizu, G.S. Simpson, P.-A. Söderström, H. Watanabe, F. Browne, P. Doornenbal, et al., β-decay half-lives of 110 neutron-rich nuclei across the $N = 82$ shell gap: implications for the mechanism and universality of the astrophysical r process, Phys. Rev. Lett. 114 (19) (2015) 192501, https://doi.org/10.1103/PhysRevLett.114.192501.

[50] C. Arlandini, F. Kappeler, K. Wisshak, R. Gallino, M. Lugaro, M. Busso, O. Straniero, Neutron capture in low-mass asymptotic giant branch stars: cross sections and abundance signatures, Astrophys. J. 525 (2) (1999) 886–900, https://doi.org/10.1086/307938, arXiv:astro-ph/9906266.

[51] S. Goriely, Uncertainties in the solar system r-abundance distribution, Astron. Astrophys. 342 (3) (1999) 881–891.

[52] C. Sneden, J.J. Cowan, R. Gallino, Neutron-capture elements in the early galaxy, Annu. Rev. Astron. Astrophys. 46 (1) (2008) 241–288, https://doi.org/10.1146/annurev.astro.46.060407.145207.

[53] B. Côté, M. Eichler, A. Yagüe, N. Vassh, M.R. Mumpower, B. Világos, B. Soós, A. Arcones, T.M. Sprouse, R. Surman, et al., 129I and 247Cm in meteorites constrain the last astrophysical source of solar r-process elements, Science 371 (6532) (2021), https://doi.org/10.1126/science.aba1111, arXiv:2006.04833, http://arxiv.org/abs/2006.04833.